

Chapter 6

Quantifying Human-Humanoid Imitation Activities

6.1 Introduction

We investigated the robustness and weaknesses of the reconstructed state spaces (RRSs) using the uniform time-delay embedding technique (UTDE) and recurrence plots (RPs) for recurrent quantification analysis (RQA) methodologies in the following conditions:

- Three levels of smoothness for the normalised data (`sg0zmuv`, `sg1zmuv` and `sg2zmuv`), computed from two different filter lengths (29 and 159) with the same polynomial degree of 5 using the function `sgolay(p,n,m)` signal R developers (2014),
- Four velocities arm movement activities: horizontal normal (HN), horizontal faster (HF), vertical normal (VN), and vertical faster (VF), and
- Four window lengths: 2-sec (100 samples), 5-sec (250 samples), 10-sec (500 samples) and 15-sec (750 samples).

Further details about the preparations of time series are presented in Section 4.6.

6.2 Time series

To make comparison easier, we only present 10-sec (500 samples) window length time series for three participants (p01, p01 and p03) performing horizontal arm movements (axis GyroZ) and vertical arm movements (axis GyroY) (Figs 6.1 and 6.2), other data is then presented in Appendix D. We consider different levels of smoothness of the normalised data with two different Savitzky-Golay filter lengths (29 and 159) with the same polynomial degree of 5 using `sgolay(p,n,m)` (signal R developers, 2014).

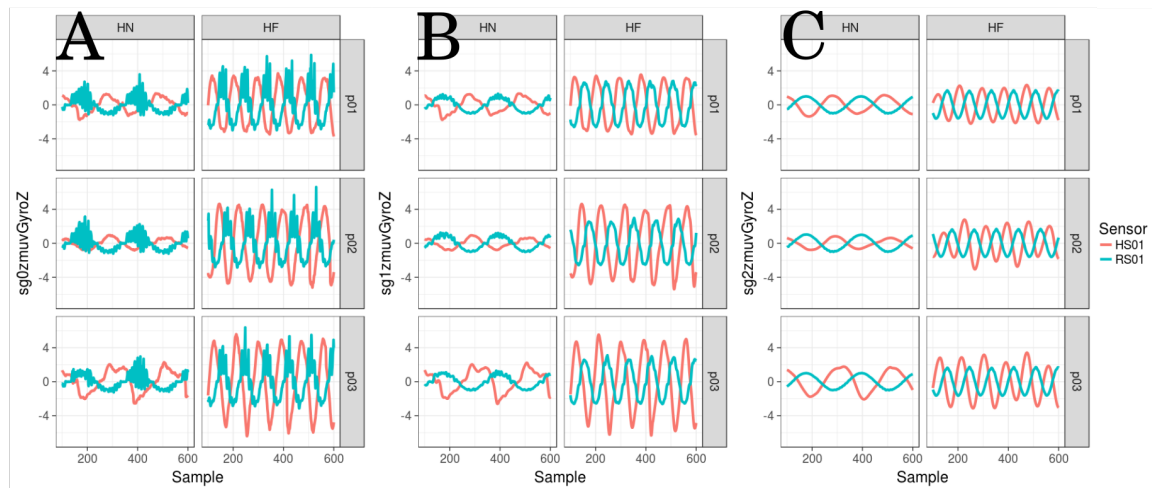


Fig. 6.1 **Time series for horizontal arm movements.** (A) raw-normalised ($sg0zmuvGyroZ$), (B) normalised-smoothed 1 ($sg1zmuvGyroZ$) and (C) normalised-smoothed 2 ($sg2zmuvGyroZ$). Time series are only for three participants (p01, p02, and p03) for horizontal movements in normal and faster velocity (HN, HF) with the normalised GyroZ axis ($zmuvGyroZ$) and with one sensor attached to the participant (HS01) and other sensor attached to the robot (RS01). R code to reproduce the figure is available from Xochicale (2018).

6.3 Minimum Embedding Parameters

The first step to create RSSs with the use of UTDE is to compute the average minimum embedding parameters for all participants, sensors and activities using False Nearest Neighbour (FNN) and Average Mutual Information algorithms (AMI).

6.3 Minimum Embedding Parameters

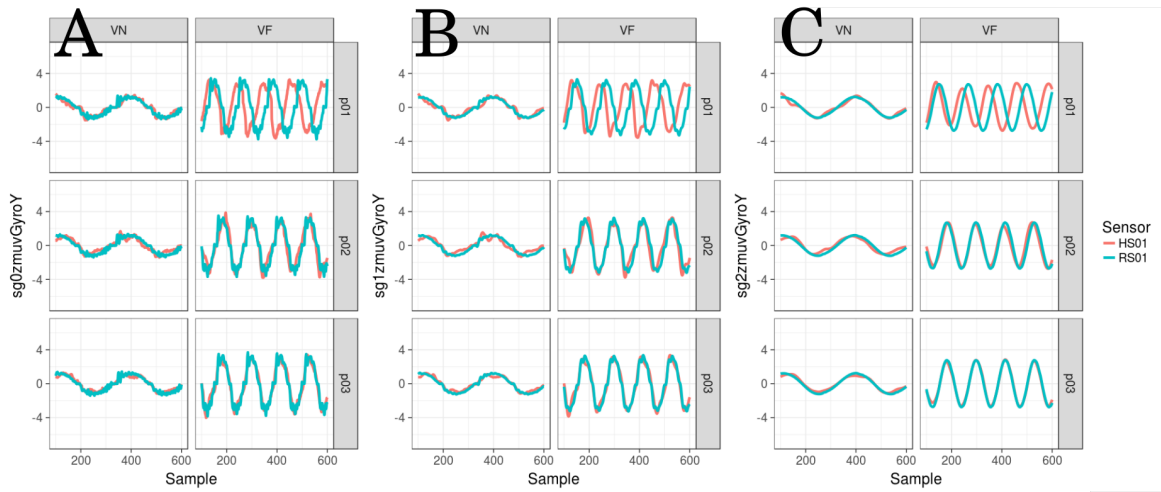


Fig. 6.2 Time series for vertical arm movements. (A) raw-normalised ($sg0zmuvGyroY$), (B) normalised-smoothed 1 ($sg1zmuvGyroY$) and (C) normalised-smoothed 2 ($sg2zmuvGyroY$). Time series are only for three participants (p01, p02, and p03) for vertical movements in normal and faster velocity (VN, VF) with the normalised GyroY axis ($zmuvGyroY$) and with one sensor attached to the participant (HS01) and other sensor attached to the robot (RS01). R code to reproduce the figure is available from Xochicale (2018).

Hence, for the average minimum embedding dimension, Figs 6.3 and 6.4 show the minimum embedding dimension for twenty participants for the horizontal and vertical arm movements at normal and faster velocity (HN, HF, VN, and VF) with the human attached sensor (HS01) and robot attached sensor (RS01). Generally, Figs 6.3 and 6.4 show that the minimum embedding values appear to be more constant for sensor RS01 than the slightly variations for embedding values for sensor HS01. It can also be seen in Figs 6.3 and 6.4 that there is a minor decrease of minimum embedding values as smoothness of time series increase.

Similarly, the first minimum values of the Average Mutual Information (AMI) for participants (p01-p20), activities (HN, HF, VN, and VF) and sensors (HS01, RS01) is shown in Figs 6.5 and 6.6. Hence, Fig 6.5(A) shows that the first minimum values of AMI, for normal horizontal arm movements, tend to be more spread as the smoothness of the time series is increasing while AMI values for faster horizontal arm movements

Quantifying Human-Humanoid Imitation Activities

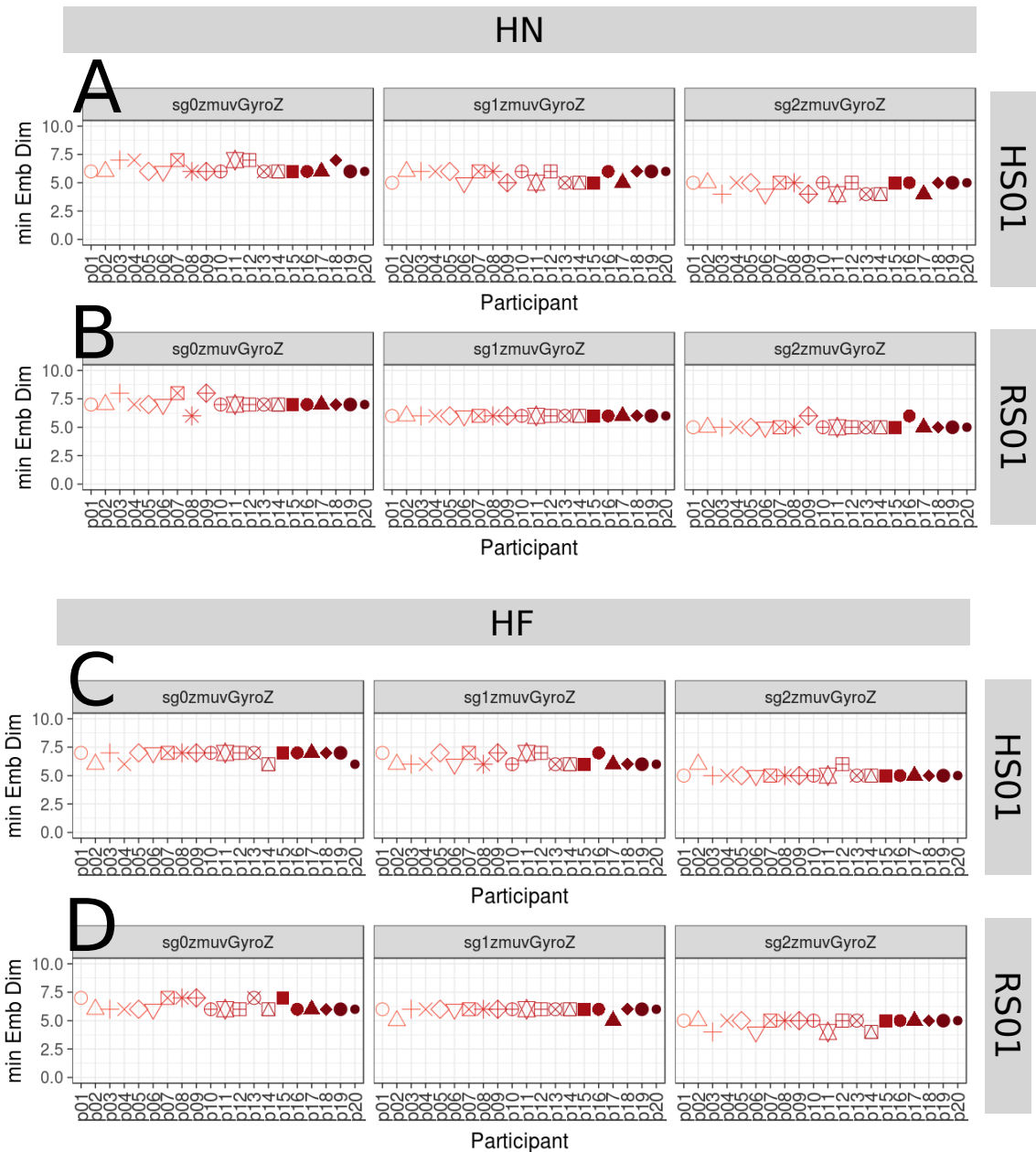


Fig. 6.3 Minimum embedding dimensions for horizontal arm movements. (A, B) Horizontal Normal (HN), (C, D) Horizontal Faster (HF) movements, (A, C) sensor attached to participants (HS01), and (B, D) sensor attached to robot (RS01). Minimum embedding dimensions are for twenty participants (p01 to p20) with three smoothed signals (sg0zmuvGyroZ, sg1zmuvGyroZ and sg2zmuvGyroZ) and window lenght of 10-sec (500 samples). R code to reproduce the figure is available from Xochicale (2018).

6.3 Minimum Embedding Parameters

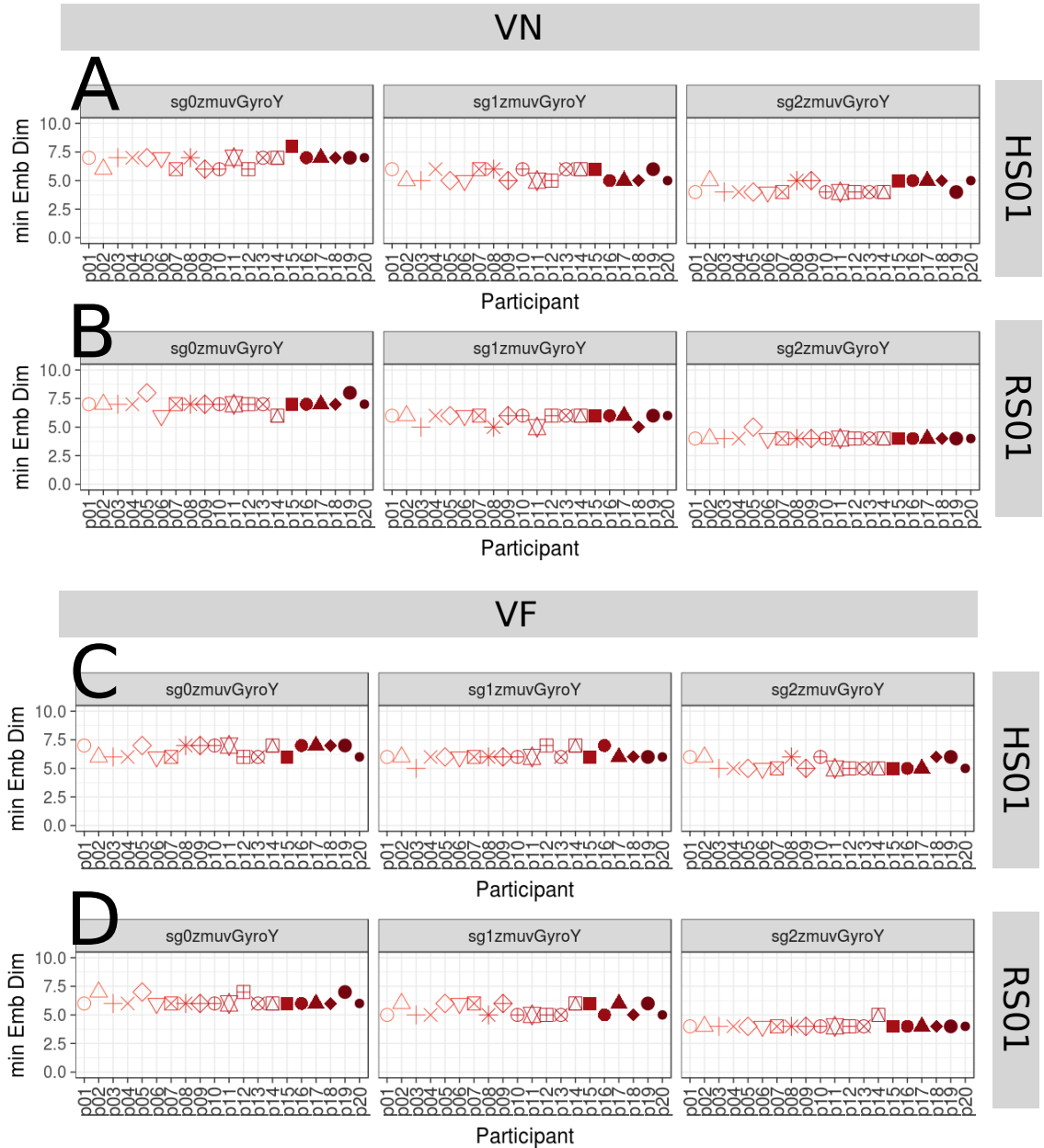


Fig. 6.4 Minimum embedding dimensions for vertical arm movements. (A, B) Vertical Normal (VN), (C, D) Vertical Faster (VF) movements, (A, C) sensor attached to participants (HS01), and (B, D) sensor attached to robot (RS01). Minimum embedding dimensions are for twenty participants (p01 to p20) with three smoothed signals (sg0zmuvGyroY, sg1zmuvGyroY and sg2zmuvGyroY) and window length of 10-sec (500 samples). R code to reproduce the figure is available from Xochicale (2018).

Quantifying Human-Humanoid Imitation Activities

in Fig 6.5(C) show little effect with regards to its fluctuation as the smoothness of time series increase. Fig 6.5(B) shows that minimum values of AMI are less spread as smoothness is increasing. However, values for horizontal faster movements in Fig 6.5(D) tend to be more spread as smoothness is increasing. With regard to vertical arm movements, the minimum values of AMI in Figs 6.6(A) and 6.6(C) show a slightly increase of the spread values as the smoothness is increasing and minimum AMI values in Fig 6.6(B) appear to have less fluctuations as the smoothness of the time series is increasing, however, that do not happen for the second smoothed values (sg2zmuvGyroY) in Fig 6.6(D) which appear to be constant. It can be noted that the increase of fluctuations of minimum AMI values in Figs 6.5 and 6.6 is due to the smoothed curves in the AMIs as the smoothness of time series is increasing.

6.4 Reconstructed state spaces with UTDE

Although the implementation of Uniform Time-Delay Embedding matrix (UTDE) is simple, the main challenge in this regard is to select embedding parameters to reconstruct the state spaces for each time series, considering that time series are unique in terms of its structure (modulation of amplitude, frequency and phase) (Bradley and Kantz, 2015; Frank et al., 2010; Samà et al., 2013). With that in mind, the problem is not to compute individual embedding parameters for each of the time series but to deal with the selection of two parameters that can represent all the time series. Our solution for that problem was, therefore, to compute a sample mean over all values that represents all participants, sensors and activities (Section 3.4.3). Hence, the sample mean for the minimum values of $E_1(m)$ from Figs 6.3 and 6.4 is $\bar{m}_0 = 6$ and the sample mean for minimum values of AMIs from Figs 6.5 and 6.6 is $\bar{\tau}_0 = 8$, for which the average minimum embedding parameters is ($\bar{m}_0 = 6$, $\bar{\tau}_0 = 8$).

6.4 Reconstructed state spaces with UTDE

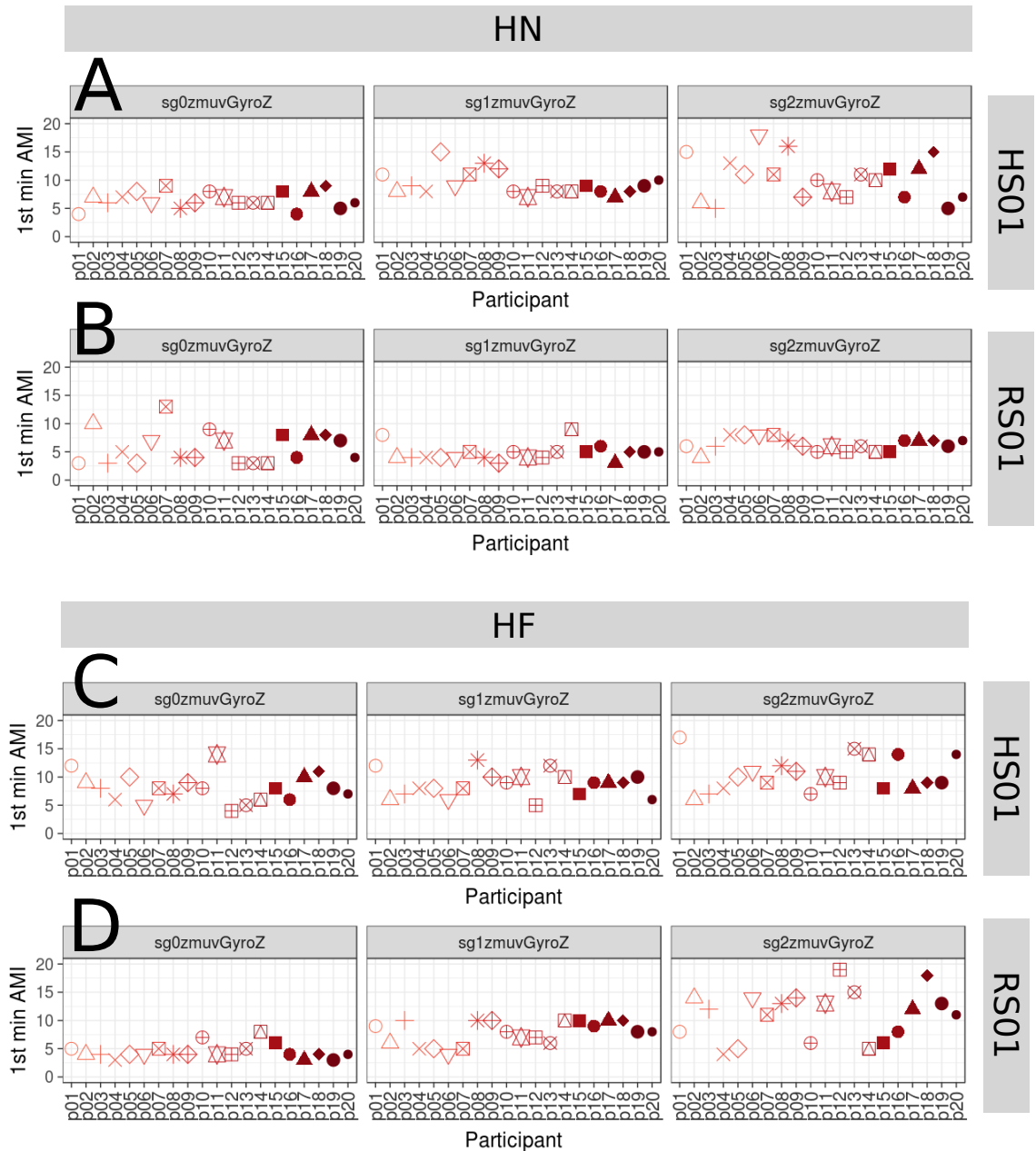


Fig. 6.5 First minimum AMI values for horizontal arm movements. (A, B) Horizontal Normal (HN), (C, D) Horizontal Faster (HF) movements, (A, C) sensor attached to participants (HS01), and (B, D) sensor attached to robot (RS01). First minimum AMI values are for twenty participants (p01 to p20) with three smoothed signals (sg0zmuvGyroZ, sg1zmuvGyroZ and sg2zmuvGyroZ) and window lenght of 10-sec (500 samples). R code to reproduce the figure is available from Xochicale (2018).

Quantifying Human-Humanoid Imitation Activities

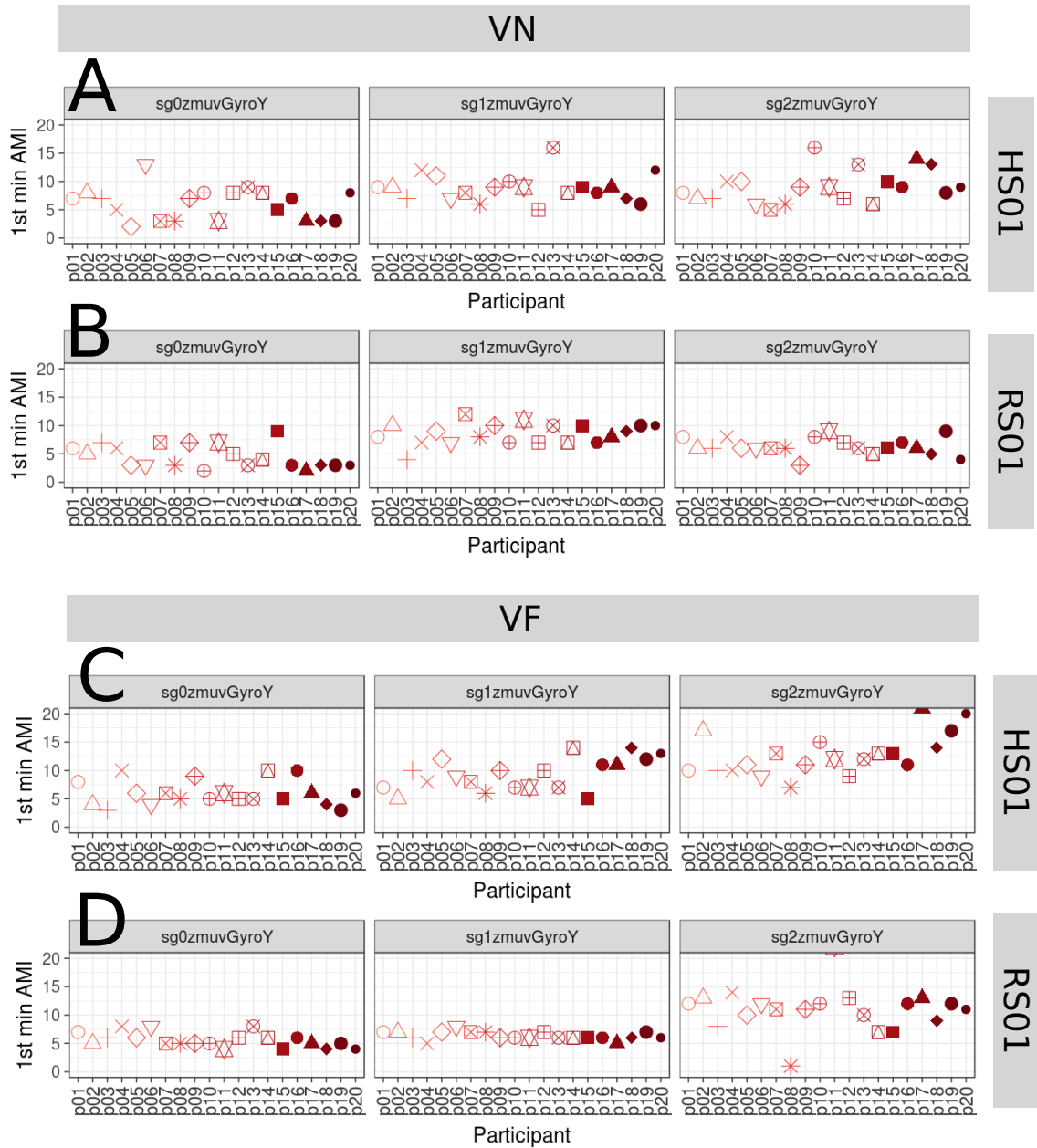


Fig. 6.6 First minimum AMI values for vertical arm movements. (A, B) Vertical Normal (VN), (C, D) Vertical Faster (VF) movements, (A, C) sensor attached to participants (HS01), and (B, D) sensor attached to robot (RS01). First minimum AMI values are for twenty participants (p01 to p20) with three smoothed signals (sg0zmuvGyroZ, sg1zmuvGyroZ and sg2zmuvGyroZ) and window lenght of 10-sec (500 samples). R code to reproduce the figure is available from Xochicale (2018).

6.4 Reconstructed state spaces with UTDE

Therefore, considering time series for participant 01 (Figs 6.1, 6.2) the reconstructed state spaces for horizontal arm movements (Figs 6.7) and vertical arm movements (Figs 6.8) are computed with $\bar{m}_0 = 6$ and $\bar{\tau}_0 = 8$ (Section 3.5).

The trajectories of the RSSs for horizontal normal and faster from the human sensors (HS01) are slightly smoothed as the time-series smoothness increase (Figs 6.7(A,C)). Similarly, the smoothness of the trajectories in the RSSs for robot sensor (RS01) is increasing as the time series smoothness increase (Figs 6.7(B,D)). Although the frequency of the movement increase from normal to faster velocity, the trajectories RSSs in Figs 6.7(B) show higher oscillations specially for a maximum values of smoothness (sg2zmuvGyroZ), while the trajectories in the RSS for HF in Figs 6.7(D) show a lower and smoothed oscillations as the smoothness increase.

In contrast, the time series for vertical movements are less noisy and well structured (Figs 6.2) for which the trajectories in the RSSs seem to be less organised, specially for Fig 6.8(A,C), while time series for vertical faster movements (VF) which have more periods (Figs 6.2), this created trajectories in the RSS with well defined patterns (6.8(C,D)). It is important to note that the smoothness of time series also create an effect on smoothness in the trajectories of the RSS, being the RS01 more organised and more persistent while trajectories for HS01 are more changeable (Figs. 6.7, 6.8).

Therefore, one can observe by eye the differences in each of the trajectories in the reconstructed state spaces (Figs 6.7, 6.8), however one might be not objective when quantifying those differences since such observations might vary from person to person. With that in mind, in our early experiments, we tried to objectively quantify those differences using euclidean distances between the origin to each of the points in the trajectories in the trajectories of the RSSs, however these created suspicious metrics, specially for trajectories which looked very messy. Hence, we considered to apply

Quantifying Human-Humanoid Imitation Activities

Recurrence Quantification Analyses in order to have a more objective quantification of the differences in each of the cases of the time series.

6.5 Recurrences Plots

With the time series of Figs 6.1 and 6.2, we computed its Recurrence Plots for horizontal arm movements (Fig 6.9) and vertical arm movements (Fig 6.10) using the average embedding parameters ($m = 6$, $\tau = 8$) and a recurrence threshold of $\epsilon = 1$. For the selection of the recurrence threshold, Marwan (2011) pointed out that choosing an appropriate recurrence threshold is crucial to get meaningful representations in the RPs, however, for this thesis where quantifying movement variability is our aim, we give little importance to the selection of the recurrence threshold for the RPs as long as it is able to represent the dynamical transitions in each of the time series.

Generally, the increase of smoothness in time series results in ticker and more well defined diagonal lines in the RPs (Figs 6.9, 6.10). Regarding the low and hight frequencies in the time series due to the changes in velocities of the movements, the patterns in the RPs show both an increase of diagonal lines and a decrease of its thickness (Figs 6.9(A,B), 6.10(C,D)). Although, the patterns of RPs show consistency with the movements type and velocities changes, it can be noticed that patterns of the RPs for HS01 are not entirely well defined while patterns of the RPs for RS01 shown a more consistent pattern (Fig 6.9, 6.10).

It is important to note that only RPs for participant 01 are presented in (Fig 6.10, 6.9), however other RPs for all participants are presented in Appendix D.4. With that in mind, we can highlight that, as similar as, the Reconstructed State Spaces (Figs 6.7, 6.8), the patterns in the RPs can be easily noticed by eye for different conditions of the time series (Figs 6.9, Fig 6.10), however these characteristics in the patterns of the RPs are subjective for the person who analysed them and might vary from person to

6.6 Recurrence Quantification Analysis

person. That lead us to apply Recurrence Quantification Analysis in order to have a more objective quantification for the movement variability for each of the conditions of the time series.

6.6 Recurrence Quantification Analysis

Considering the RPs for 20 participants performing four activities (HN, HF, VN and VF) with sensors attached to the human (HS01) and to the humanoid robot (RS01) and with the increase of smoothness ($sg0zmuvGyroZ$, $sg1zmuvGyroZ$ and $sg2zmuvGyroZ$), we hence compute four metrics of RQA metrics (REC, DET, RATIO and ENTR) with embedding parameters $m = 6$, $\tau = 8$ and recurrence threshold $\epsilon = 1$ shown in the following subsections.

6.6.1 REC values

It can be seen in Figs 6.11 and 6.12 that REC values, representing the % of black dots in the RPs, are more spread for HN than HF movements with time series coming from HS01 sensor. In contrast, REC values appear to be constant and present little variation for both HN and HF movements with time series from the sensor attached to the humanoid robot RS01. With regard to the increase of smoothness of time series ($sg0zmuvGyroZ$, $sg1zmuvGyroZ$ and $sg2zmuvGyroZ$), REC values present little variation as the smoothness is increasing for time series from HS01 and REC values more similar as the smoothness is increasing for data from RS01.

6.6.2 DET values

DET values, representing predictability and organisation of the RPs, change very little even for type of movement and type of sensor (Figs 6.13 and 6.14). With regard to the

Quantifying Human-Humanoid Imitation Activities

smoothness of time series, DET values appear to be more similar as the smoothness of the time series is increasing.

6.6.3 RATIO values

RATIO values, representing dynamic transitions, for both horizontal and vertical movements (Figs 6.15 and 6.16) vary less for HN movements than HF movements for HS01 sensor which is a similar behaviour of RATIO values for RS01 sensor. It can also noticed a decrease of variation in RATIO values as the smoothness of the time series is increasing.

6.6.4 ENTR values

ENTR values, representing the complexity of the deterministic structure of the time series, for both horizontal and vertical movements (Figs 6.17 and 6.18) show more variation for HS01 sensor than ENTR values for RS01 sensor which appear to be more constant. Generally, it can also be said that the smoothness of time series affects little to the variation of ENTR values.

6.7 The weaknesses and strengths of RQA

Considering the raised points in Section 3.7.4 regarding the weaknesses and strengths of RQA, we computed RQA metrics (REC, DET, RATIO and ENTR) and plotted 3D surfaces using an unitary increase of pair embedding parameters ($0 > m \leq 10$, $0 > \tau \leq 10$) and a decimal increase of 0.1 for recurrence thresholds ($0.2 \geq \epsilon \leq 3$) (Fig. 6.19). Hence, the 3D surface for REC values, representing the percentage of black dots in the RP, in Fig. 6.19(A) shows an increase for REC values as the recurrence threshold increase, while the variation for embedding parameters creates

6.7 The weaknesses and strengths of RQA

slightly decrease of REC values as the dimension m increase and even a more slighter decrements of REC values for the increase of τ . For the 3D surface of DET values (Fig. 6.19(B)), representing predictability and organisation of the RPs, can be noted a plateau for DET values near to 1 for embedding dimension parameters of less than 5 and recurrence threshold values of greater than 2. It can also be noted that the increases of delay embedding made the DET values increase so as to make an cascade effect in the surface along with the increase of dimension embedding m . For RATIO values (Fig. 6.19(C)), representing dynamic transitions, the 3D surface show a plateau of RATIO values near to zero for recurrence thresholds greater than 1.0, while fluctuations are more evident for recurrence thresholds of less than 1.0, particularly it can also be noted an increase in the fluctuations of RATIO values as the embedding dimension is increasing. For ENTR values in Fig. 6.19(D), representing the complexity of the deterministic structure in time series, it can be noted that the increase of recurrence threshold is, not strictly linearly, proportional to the increase of ENTR values. It can also be seen that the increase of delay embeddings affects little the ENTR values for embedding dimensions of 1, while for higher values of embedding dimensions there is a decrease of ENTR values as the increase of the embedding dimension, besides the decrease of ENTR values as delay dimension value is increasing.

6.7.1 Sensors and activities

We also computed 3D surfaces of RQA metrics for different sensors and different activities (Figs. 6.20, 6.21), where it can generally be noted similar 3D surface patterns for RQA metrics as the ones in Fig. 6.19.

The 3D surfaces for REC values (Fig. 6.20(A)) show slightly differences with regard to vertical or horizontal activities however there are notable differences for normal and faster velocities, specially for the faster movements where the 3D surfaces shown a

Quantifying Human-Humanoid Imitation Activities

maximum REC value for embedding dimension values near to 1 and for recurrence thresholds near to 3. The 3D surfaces for DET values (Fig. 6.20(B)) and RATIO values (Fig. 6.20(C)) show slightly notable variations across the type of activities. For 3D surfaces of ENTR values it can be noted a slightly variation for the surfaces of normal and faster velocities (Fig 6.20(D)).

As similar as Fig 6.20, the 3D surfaces patterns for RS01 in Fig 6.21 show the differences between the activities performed at normal and faster velocities specially for REC and ENTR values (Fig 6.20(A, D)), while 3D surfaces for DET and RATIO values show slightly variations (Fig 6.20(B, C)).

6.7.2 Window size

3D surfaces for RQA metrics with four window size lengths of 100, 250, 500 and 750 samples are shown in Fig. 6.22. In general, the increase of samples in the time series creates 3D surface patterns with better resolution (Figs. 6.22).

6.7.3 Smoothness

Considering three levels of smoothness of the time series (sg0, sg1, sg2) to compute the 3D surfaces of the RQA metrics, it can be noted that such smoothness have a direct effect on the smoothness of the 3D surfaces. Especially for dimension embeddings lower than 2 with the increase of delay embedding which is more evident for REC and ENTR values (Fig. 6.23(A, D)). The 3D surfaces of DET values are smoothed to a degree that the plateau is increase, while RATIO values appear to be less affected to the level of smoothness (Fig. 6.23(C)).

6.7.4 Participants

3D surfaces of RQA metrics were also computed for three participants (Fig. 6.24). Differences of the 3D surfaces across participants are more notable with REC (Fig. 6.24(A)) and ENTR values (Fig. 6.24(D)), while minor differences of 3D surfaces across participants are presented in DET (Fig. 6.24B)) and RATIO vales (Fig. 6.24(C)).

6.7.5 Final remarks

Generally, it can be noted the changes for RQA metrics are evident with both the increase of embedding dimension parameters and the recurrence threshold for different structures, window size, levels of smoothness of the time series. RATIO values present a plateau (blue colour surface) which is independently to the source of time series, however there are peaks that change differently based on the source of time series for embedding parameters increasing with recurrence threshold less than one. For DET values, 3D surfaces present a fluctuated surface (red colour) which slightly differs with the source of time series. With regards to REC values, 3D surfaces are affected with the type of velocity, for instance, surfaces for normal velocity presents an increase of REC values as recurrence threshold increase and keeping slightly uniform surface changes for the increase of embedding parameters, however for faster velocity the 3D surface fluctuations decrease as the embedding dimension increase and recurrence thresholds increase. Similar as the human-image activities, 3D surfaces for ENTR values in this experiment present changes for any source of time series, making ENTR values a robust metric to quantify human-humanoid activities for analysis of movements variability from different time series.

Quantifying Human-Humanoid Imitation Activities

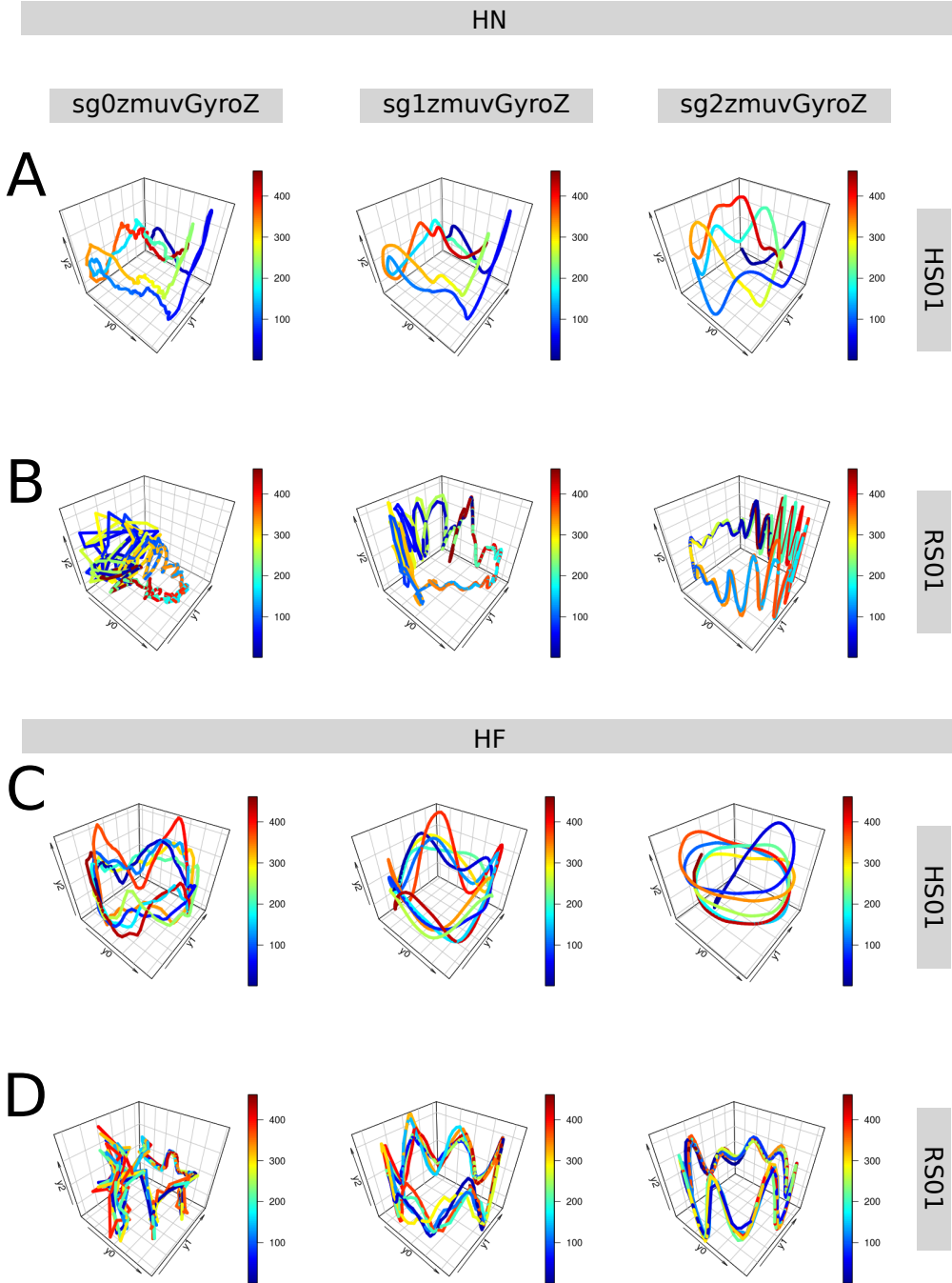


Fig. 6.7 RSSs for horizontal arm movements. Reconstructed state spaces of participant p01 for horizontal movements in normal and faster velocity (HN, HF) with raw-normalised ($sg0zmuvGyroZ$), normalised-smoothed 1 ($sg1zmuvGyroZ$) and normalised-smoothed 2 ($sg2zmuvGyroZ$) time series of the sensors attached to the participant (HS01) and other sensor attached to the robot (RS01). Reconstructed state spaces were computed with embedding parameters $m = 6$, $\tau = 8$. R code to reproduce the figure is available from Xochicale (2018).

6.7 The weaknesses and strengths of RQA

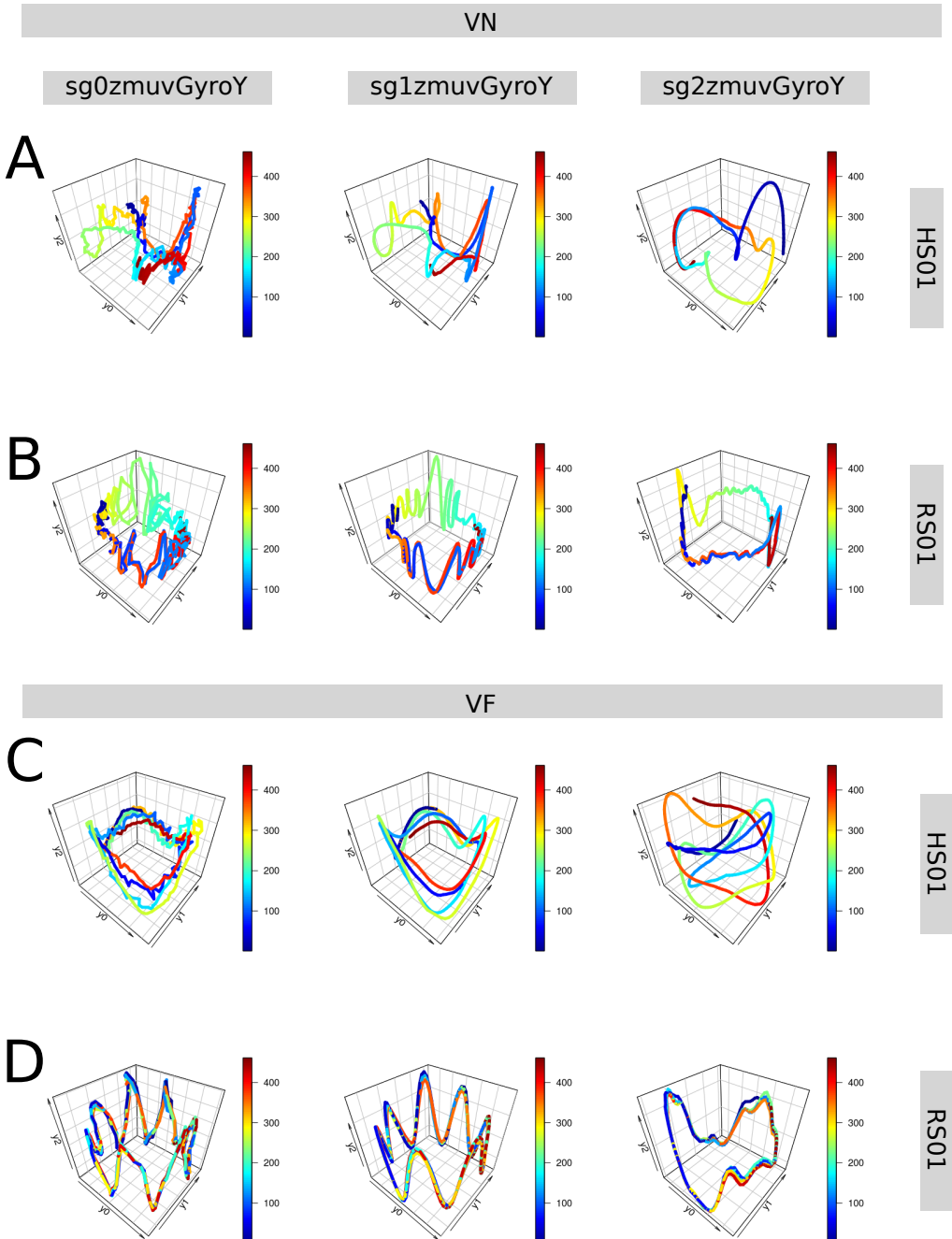


Fig. 6.8 RSSs for vertical arm movements. Reconstructed state spaces of participant p01 for vertical movements in normal and faster velocity (VN, VF) with raw-normalised ($sg0zmuvGyroZ$), normalised-smoothed 1 ($sg1zmuvGyroZ$) and normalised-smoothed 2 ($sg2zmuvGyroZ$) time series of the sensors attached to the participant (HS01) and other sensor attached to the robot (RS01). Reconstructed state spaces were computed with embedding parameters $m = 6$, $\tau = 8$. R code to reproduce the figure is available from Xochicale (2018).

Quantifying Human-Humanoid Imitation Activities

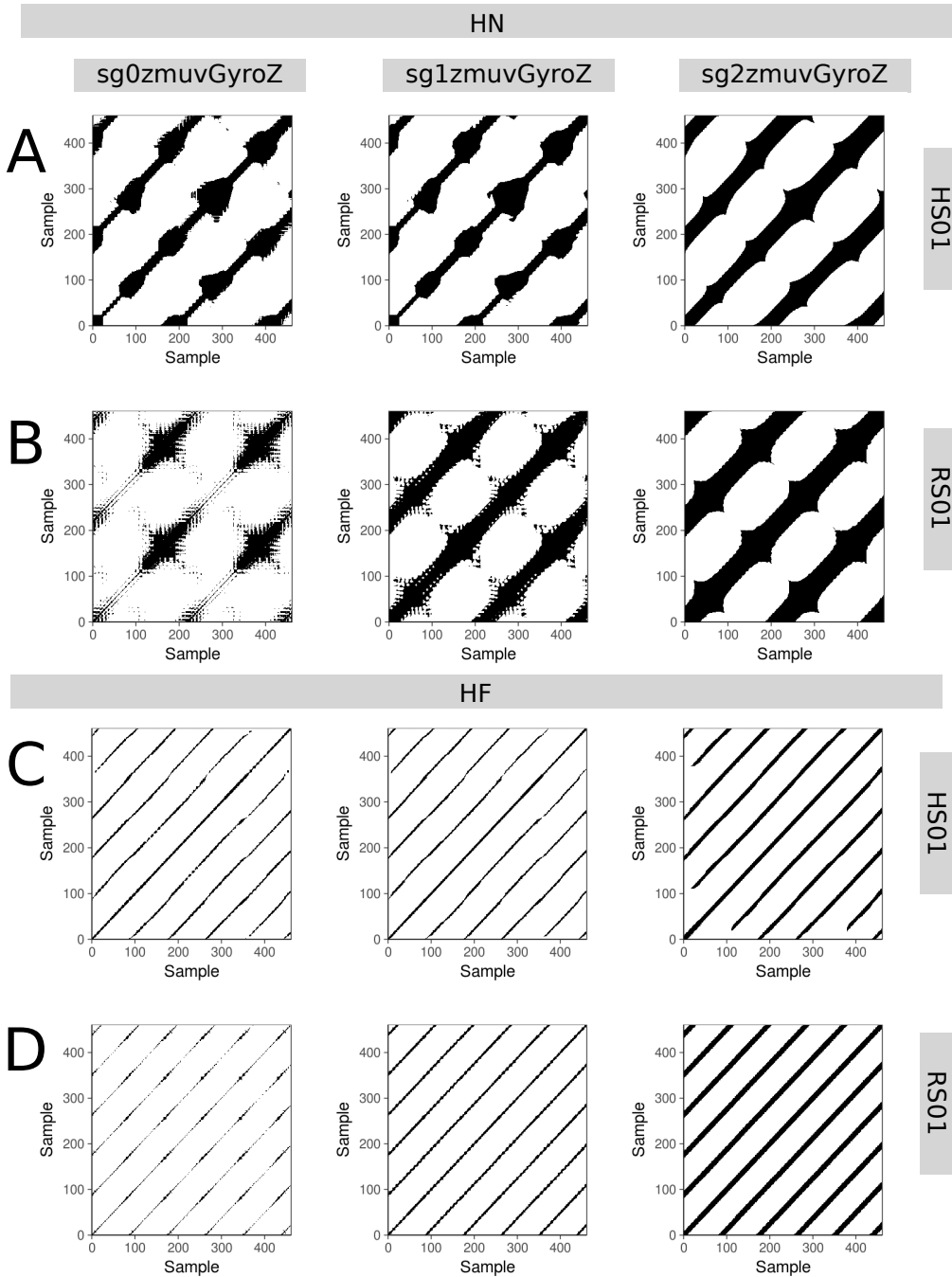


Fig. 6.9 RPs for horizontal arm movements. Recurrence plots of participant p01 for horizontal movements in normal and faster velocity (HN, HF) with raw-normalised ($sg0zmuvGyroZ$), normalised-smoothed 1 ($sg1zmuvGyroZ$) and normalised-smoothed 2 ($sg2zmuvGyroZ$) time series of the sensors attached to the participant (HS01) and other sensor attached to the robot (RS01). Recurrence plots were computed with embedding parameters $m = 6$, $\tau = 8$ and $\epsilon = 1$. R code to reproduce the figure is available from Xochicale (2018).

6.7 The weaknesses and strengths of RQA

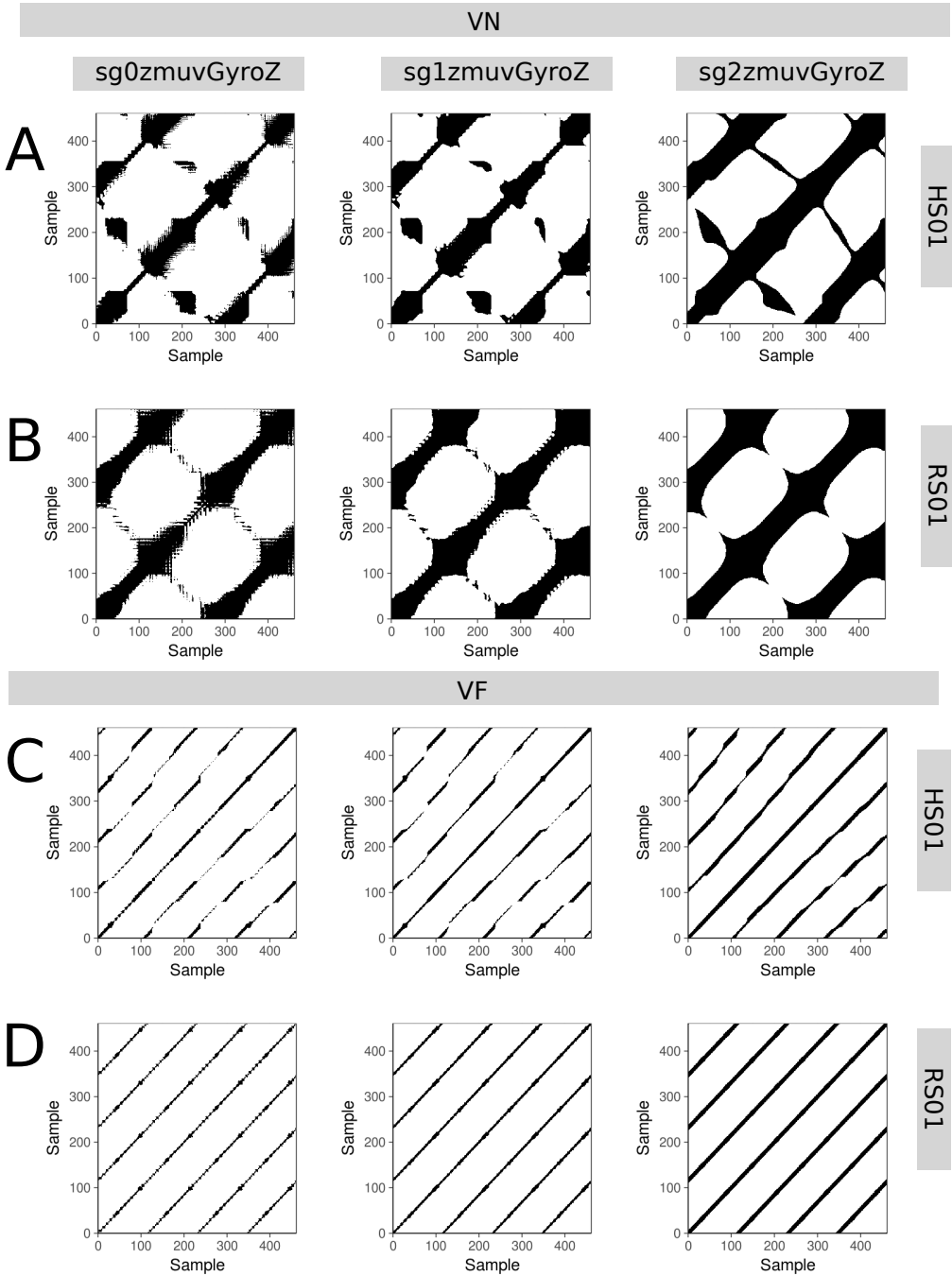


Fig. 6.10 RPs for vertical arm movements. Recurrence plots of participant p01 for vertical movements in normal and faster velocity (VN, VF) with raw-normalised ($sg0zmuvGyroZ$), normalised-smoothed 1 ($sg1zmuvGyroZ$) and normalised-smoothed 2 ($sg2zmuvGyroZ$) time series of the sensors attached to the participant (HS01) and other sensor attached to the robot (RS01). Recurrence plots were computed with embedding parameters $m = 6$, $\tau = 8$ and $\epsilon = 1$. R code to reproduce the figure is available from Xochicale (2018).

Quantifying Human-Humanoid Imitation Activities

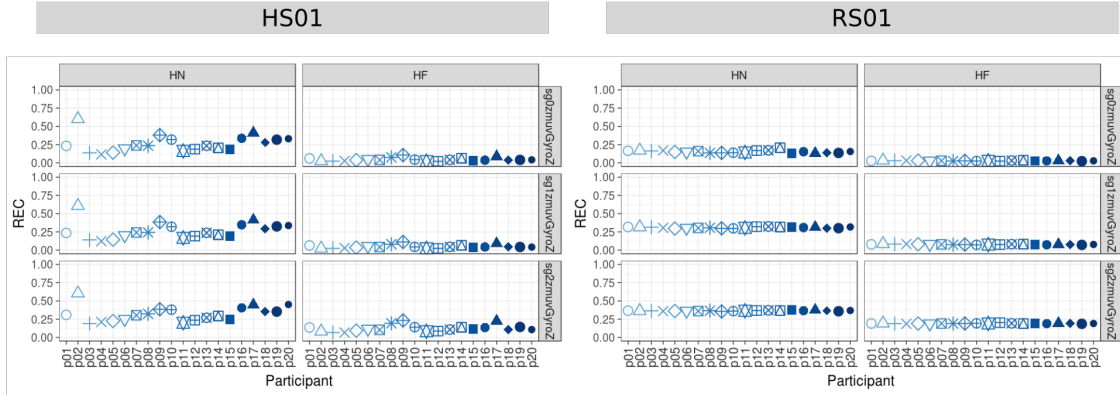


Fig. 6.11 REC values for horizontal arm movements. REC values (representing % of black dots in the RPs) for 20 participants performing HN and HF movements with sensors HS01, RS01 and three smoothed-normalised axis of GyroZ (sg0zmuvGyroZ, sg1zmuvGyroZ and sg2zmuvGyroZ). REC values were computed with embedding parameters $m = 6$, $\tau = 8$ and $\epsilon = 1$. R code to reproduce the figure is available from Xochicale (2018).

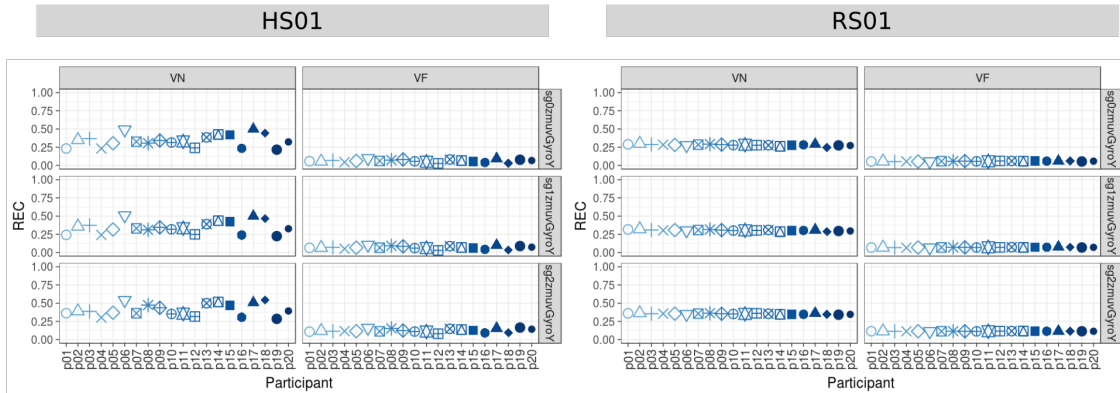


Fig. 6.12 REC values for vertical arm movements. REC values (representing % of black dots in the RPs) for 20 participants performing VN and VF movements with sensors HS01, RS01 and three smoothed-normalised axis of GyroY (sg0zmuvGyroY, sg1zmuvGyroY and sg2zmuvGyroY). REC values were computed with embedding parameters $m = 6$, $\tau = 8$ and $\epsilon = 1$. R code to reproduce the figure is available from Xochicale (2018).

6.7 The weaknesses and strengths of RQA

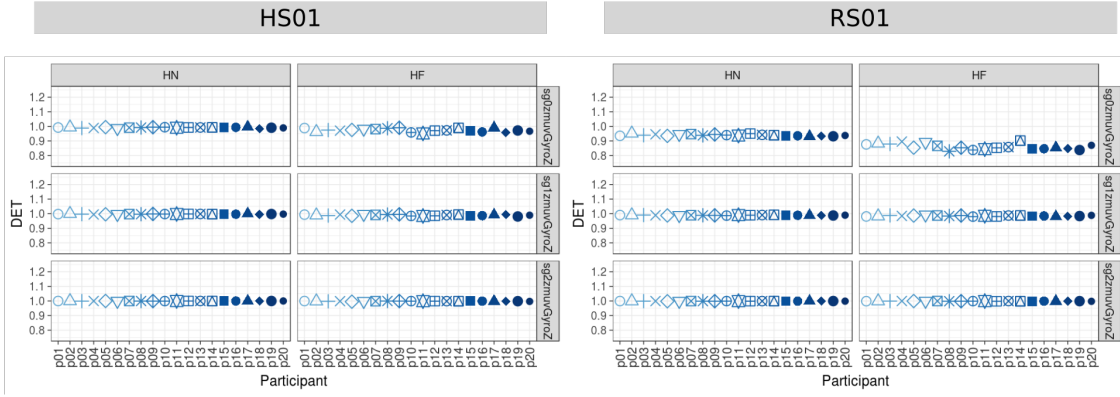


Fig. 6.13 **DET values for horizontal arm movements.** DET values (representing predictability and organisation of the RPs) for 20 participants performing HN and HF movements with sensors HS01, RS01 and three smoothed-normalised axis of GyroZ (sg0zmuvGyroZ, sg1zmuvGyroZ and sg2zmuvGyroZ). DET values were computed with embedding parameters $m = 6$, $\tau = 8$ and $\epsilon = 1$. R code to reproduce the figure is available from Xochicale (2018).

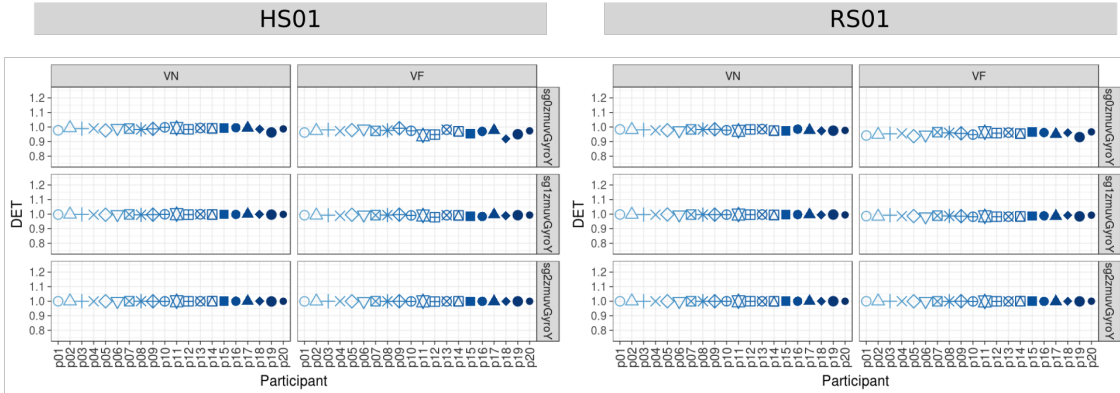


Fig. 6.14 **DET values for vertical arm movements.** DET values (representing predictability and organisation of the RPs) for 20 participants performing VN and VF movements with sensors HS01, RS01 and three smoothed-normalised axis of GyroY (sg0zmuvGyroY, sg1zmuvGyroY and sg2zmuvGyroY). DET values were computed with embedding parameters $m = 6$, $\tau = 8$ and $\epsilon = 1$. R code to reproduce the figure is available from Xochicale (2018).

Quantifying Human-Humanoid Imitation Activities

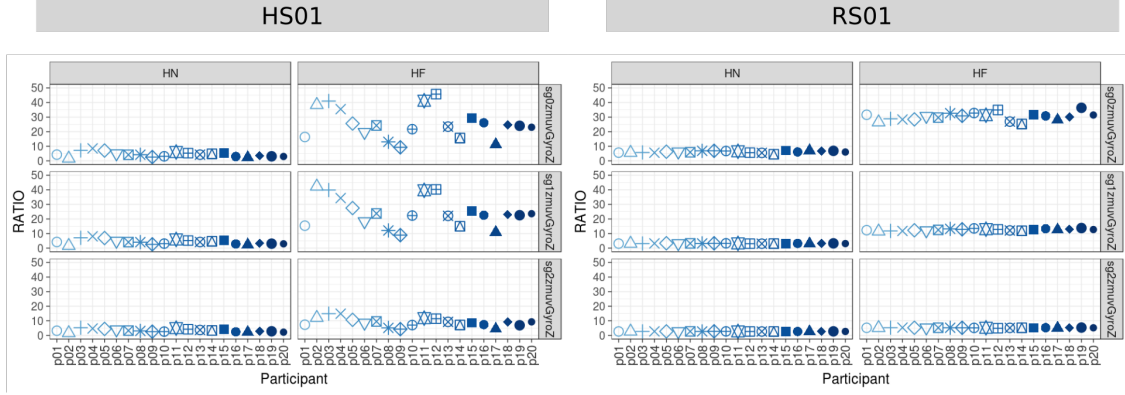


Fig. 6.15 RATIO values for horizontal arm movements. RATIO (representing dynamic transitions) for 20 participants performing HN and HF movements with sensors HS01, RS01 and three smoothed-normalised axis of GyroZ (sg0zmuvGyroZ, sg1zmuvGyroZ and sg2zmuvGyroZ). RATIO values were computed with embedding parameters $m = 6$, $\tau = 8$ and $\epsilon = 1$. R code to reproduce the figure is available from Xochicale (2018).

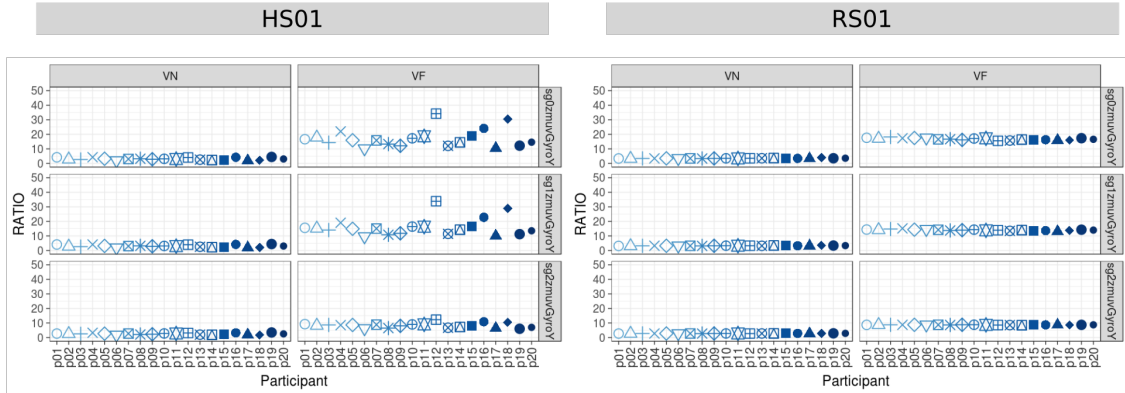


Fig. 6.16 RATIO values for vertical arm movements. RATIO (representing dynamic transitions) for 20 participants performing VN and VF movements with sensors HS01, RS01 and three smoothed-normalised axis of GyroY (sg0zmuvGyroY, sg1zmuvGyroY and sg2zmuvGyroY). RATIO values were computed with embedding parameters $m = 6$, $\tau = 8$ and $\epsilon = 1$. R code to reproduce the figure is available from Xochicale (2018).

6.7 The weaknesses and strengths of RQA

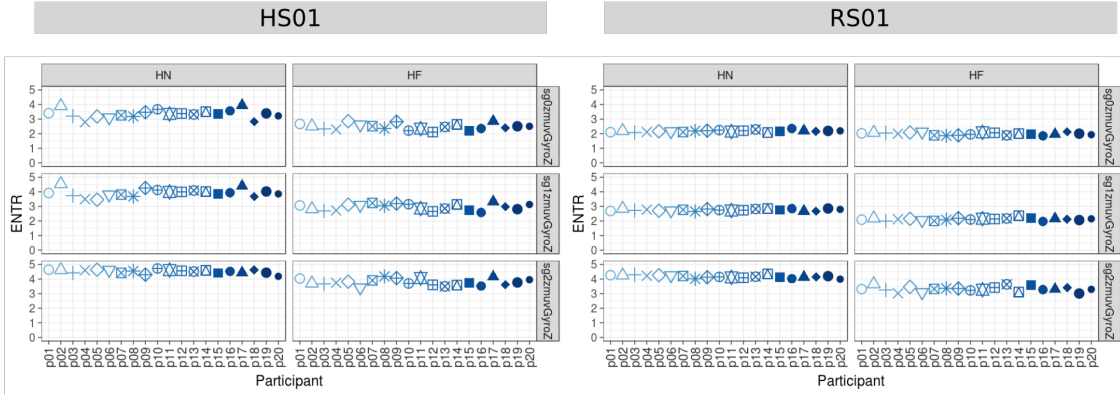


Fig. 6.17 ENTR values for horizontal arm movements. ENTR values (representing the complexity of the deterministic structure in time series) for 20 participants performing HN and HF movements with sensors HS01, RS01 and three smoothed-normalised axis of GyroZ (sg0zmuvGyroZ, sg1zmuvGyroZ and sg2zmuvGyroZ). ENTR values were computed with embedding parameters $m = 6$, $\tau = 8$ and $\epsilon = 1$. R code to reproduce the figure is available from Xochicale (2018).

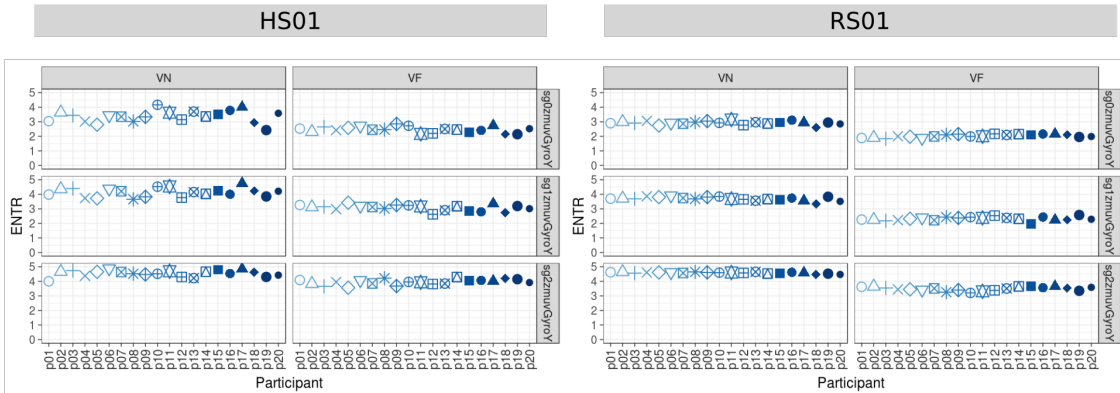


Fig. 6.18 ENTR values for vertical arm movements. ENTR values (representing the complexity of the deterministic structure in time series) for 20 participants performing VN and VF movements with sensors HS01, RS01 and three smoothed-normalised axis of GyroY (sg0zmuvGyroY, sg1zmuvGyroY and sg2zmuvGyroY). ENTR values were computed with embedding parameters $m = 6$, $\tau = 8$ and $\epsilon = 1$. R code to reproduce the figure is available from Xochicale (2018).

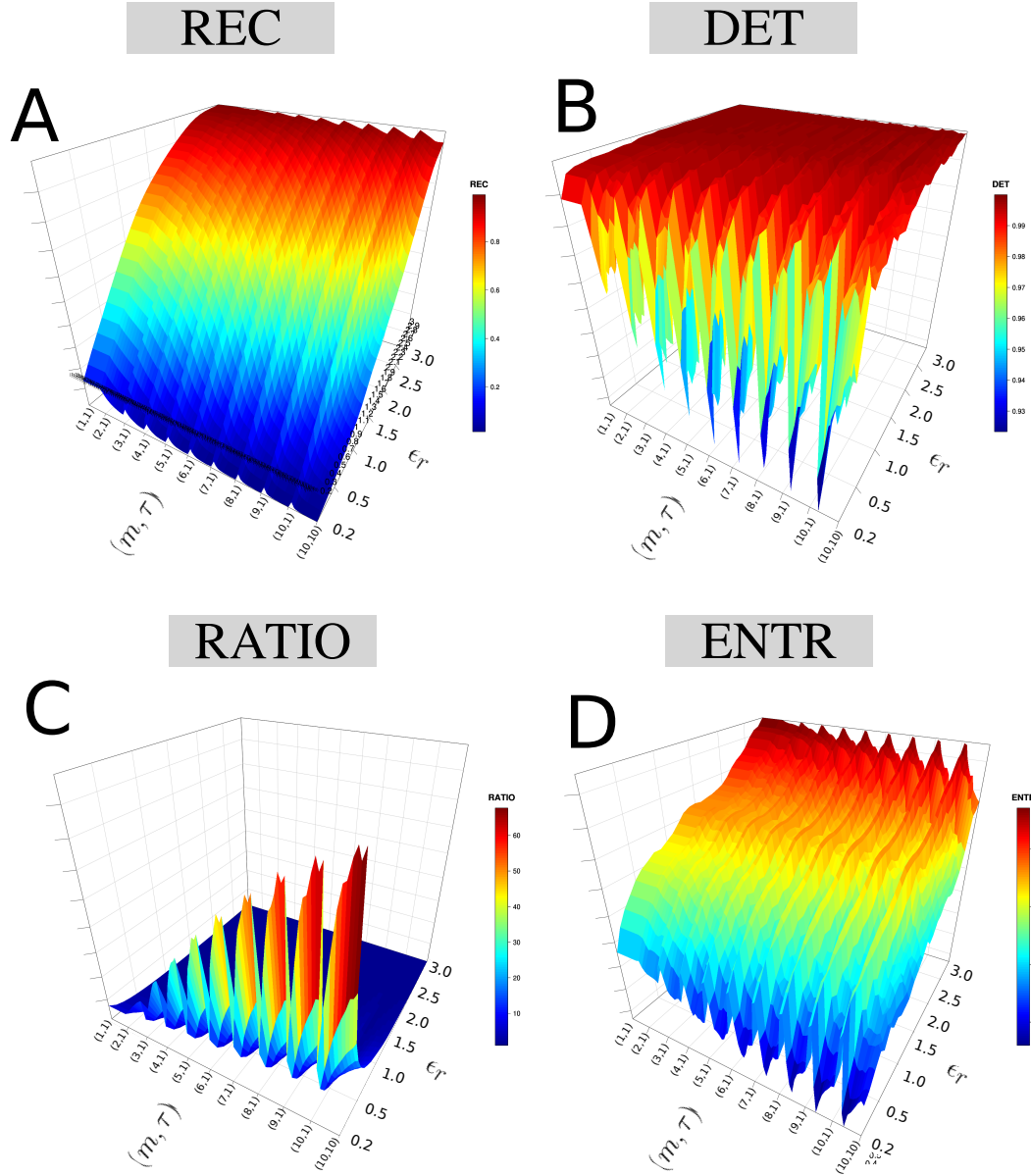


Fig. 6.19 **3D surfaces for RQA metrics.** 3D surfaces for (A) REC, (B) DET, (C) RATIO and (D) ENTR values with increasing pair of embedding parameters ($0 \leq m \leq 10$, $0 \leq \tau \leq 10$) and recurrence thresholds ($0.2 \geq \epsilon \leq 3$). RQA metrics are computed with the time series of participant *p01* using HS01 sensor, HN activity, sg0zmuvGyroZ axis and 500 samples for window size length. R code to reproduce the figure is available from Xochicale (2018).

6.7 The weaknesses and strengths of RQA

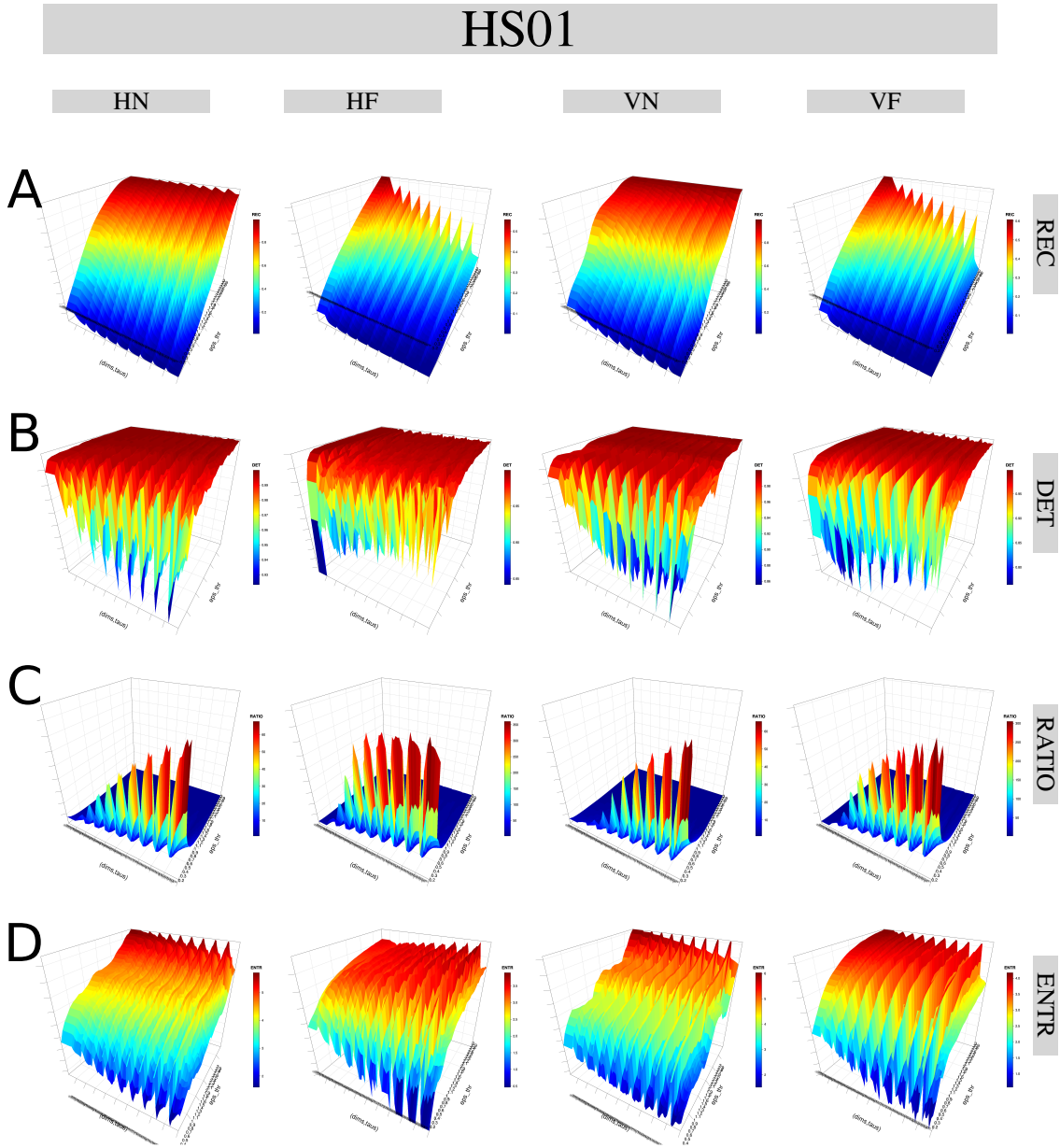


Fig. 6.20 3D surfaces of RQA metrics for HS01 sensor. 3D surfaces of RQA metrics ((A) REC, (B) DET, (C) RATIO, and (D) ENTR) with increasing embedding parameters and recurrence thresholds are for time series of participant *p01* for sensors HS01, activities (HN, HF, VN and VF) and sg0zmuvGyroZ axis with 500 samples window size length. R code to reproduce the figure is available from Xochicale (2018).

Quantifying Human-Humanoid Imitation Activities

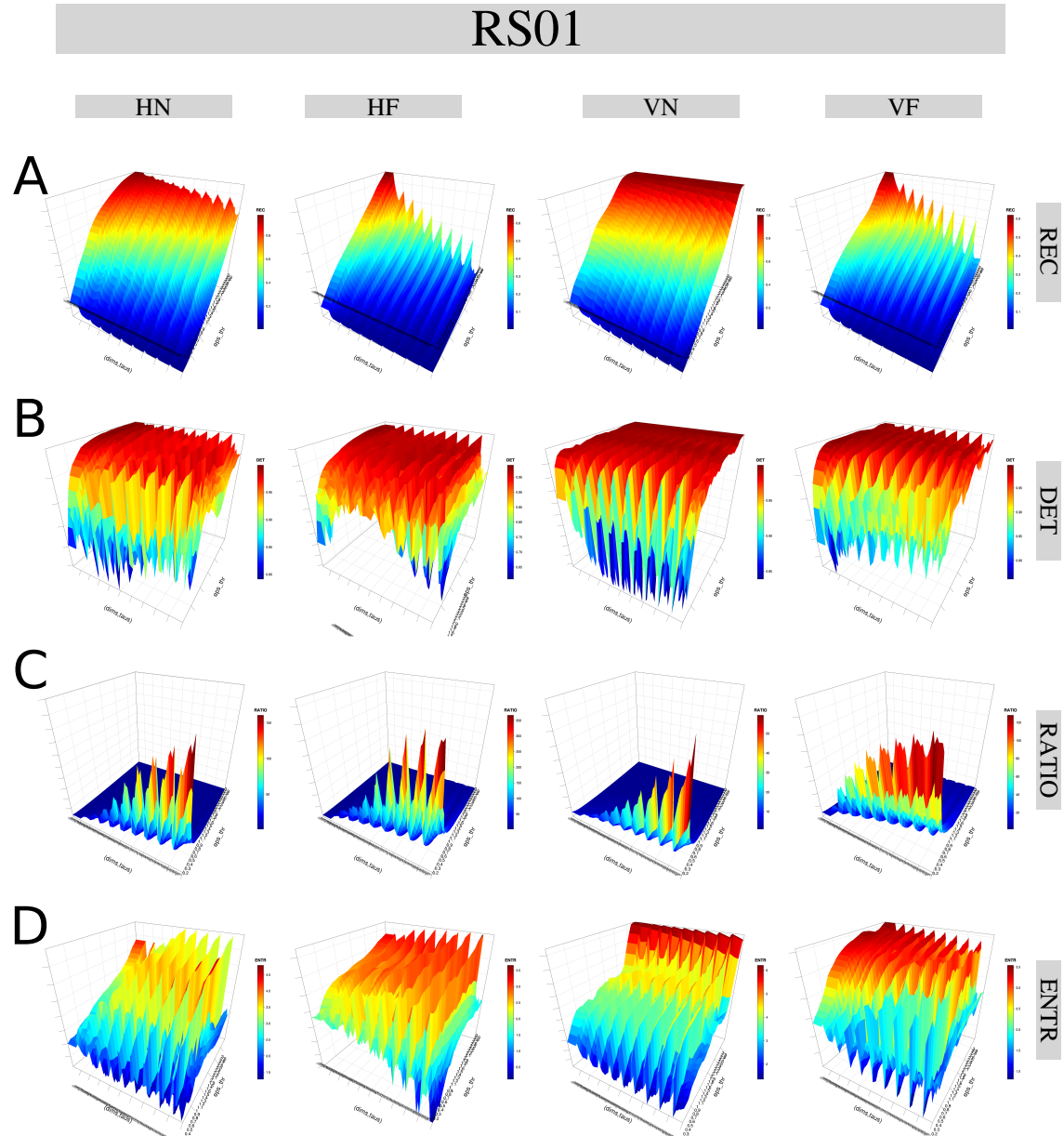


Fig. 6.21 **3D surfaces of RQA metrics for RS01 sensor.** 3D surfaces of RQA metrics ((A) REC, (B) DET, (C) RATIO and (D) ENTR) with increasing embedding parameters and recurrence thresholds are for time series of humanoid robot for sensors RS01, activities (HN, HF, VN and VF) and sg0zmuvGyroZ axis with 500 samples window size length. R code to reproduce the figure is available from Xochicale (2018).

6.7 The weaknesses and strengths of RQA

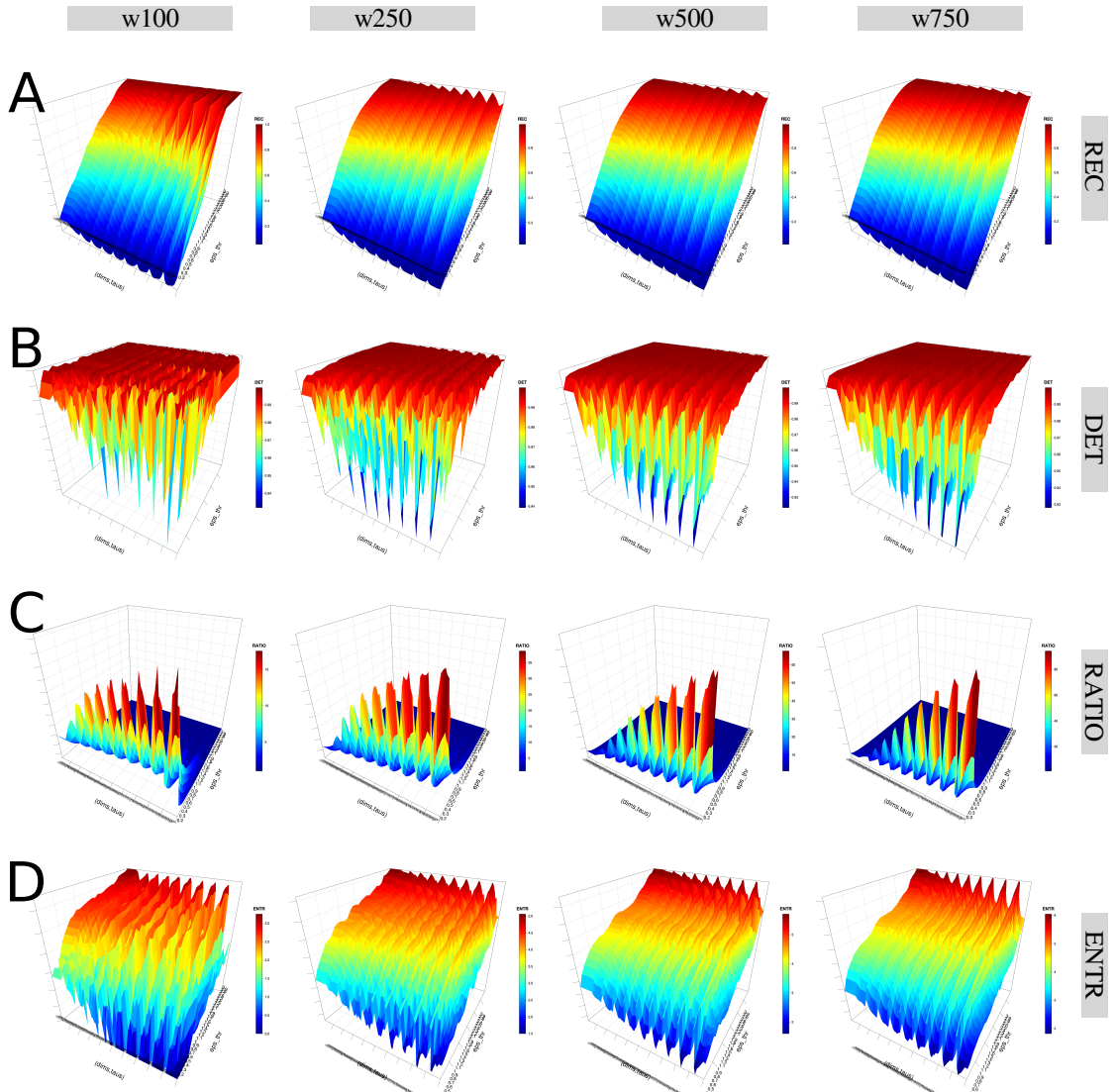


Fig. 6.22 3D surfaces for RQAs metrics with four window lengths. 3D surfaces of RQA metrics ((A) REC, (B) DET, (C) RATIO, and (D) ENTR) with increasing embedding parameters and recurrence thresholds for four window lengths (w100, w250, w500 and w750). RQA metrics values are for time series of participant *p01* using HS01 sensor, HN activity and sg0zmuvGyroZ axis. R code to reproduce the figure is available from Xochicale (2018).

Quantifying Human-Humanoid Imitation Activities

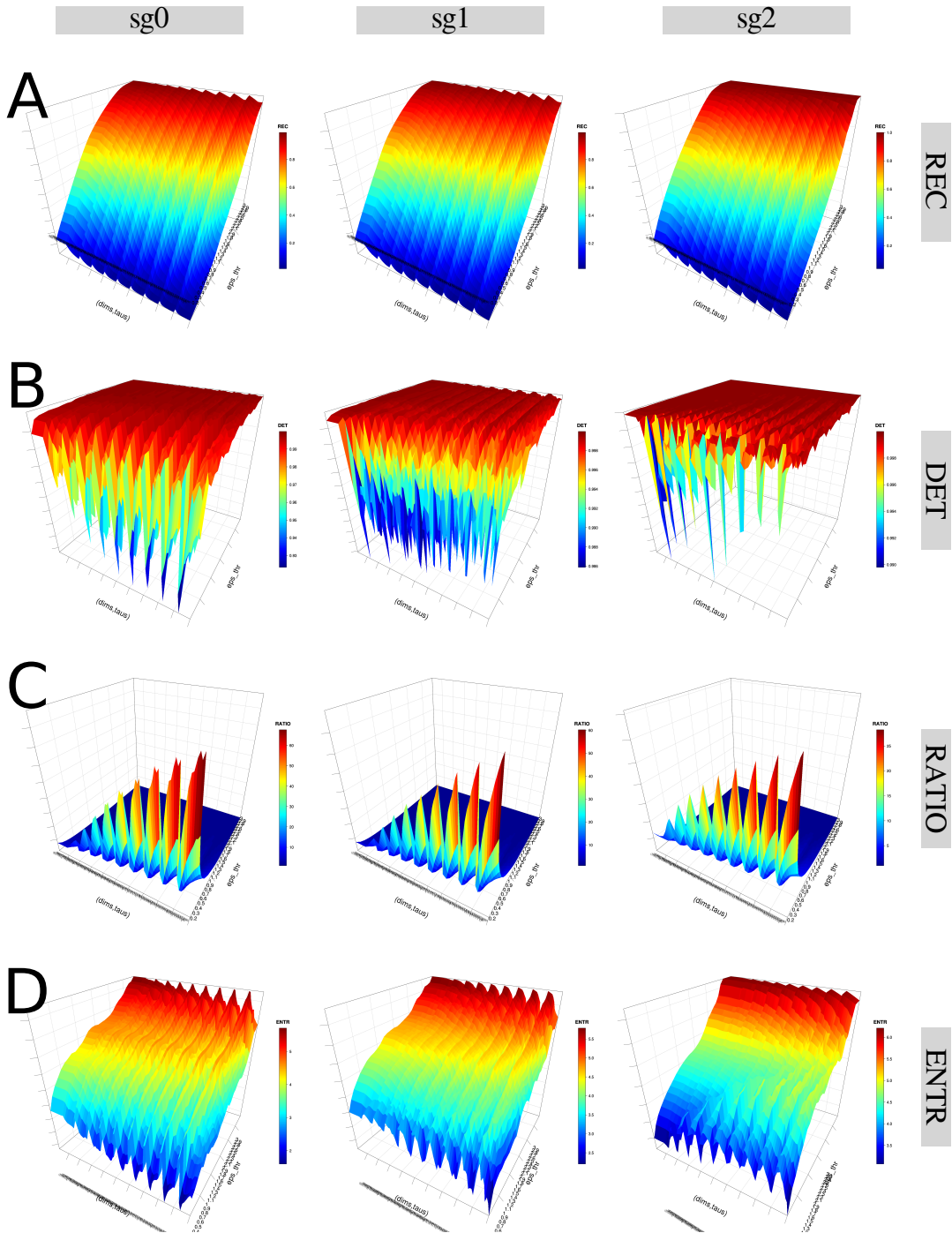


Fig. 6.23 3D surfaces for RQA metrics with three levels of smoothness. 3D surfaces of RQA metrics ((A) REC, (B) DET, (C) RATIO, and (D) ENTR) with increasing embedding parameters and recurrence thresholds for three levels of smoothness (sg0zmuvGyroZ, sg1zmuvGyroZ and sg1zmuvGyroZ). RQA metrics are computed from time series of participant *p01* using HS01 sensor, HN activity and 500 samples window length. R code to reproduce the figure is available from Xochicale (2018).

6.7 The weaknesses and strengths of RQA

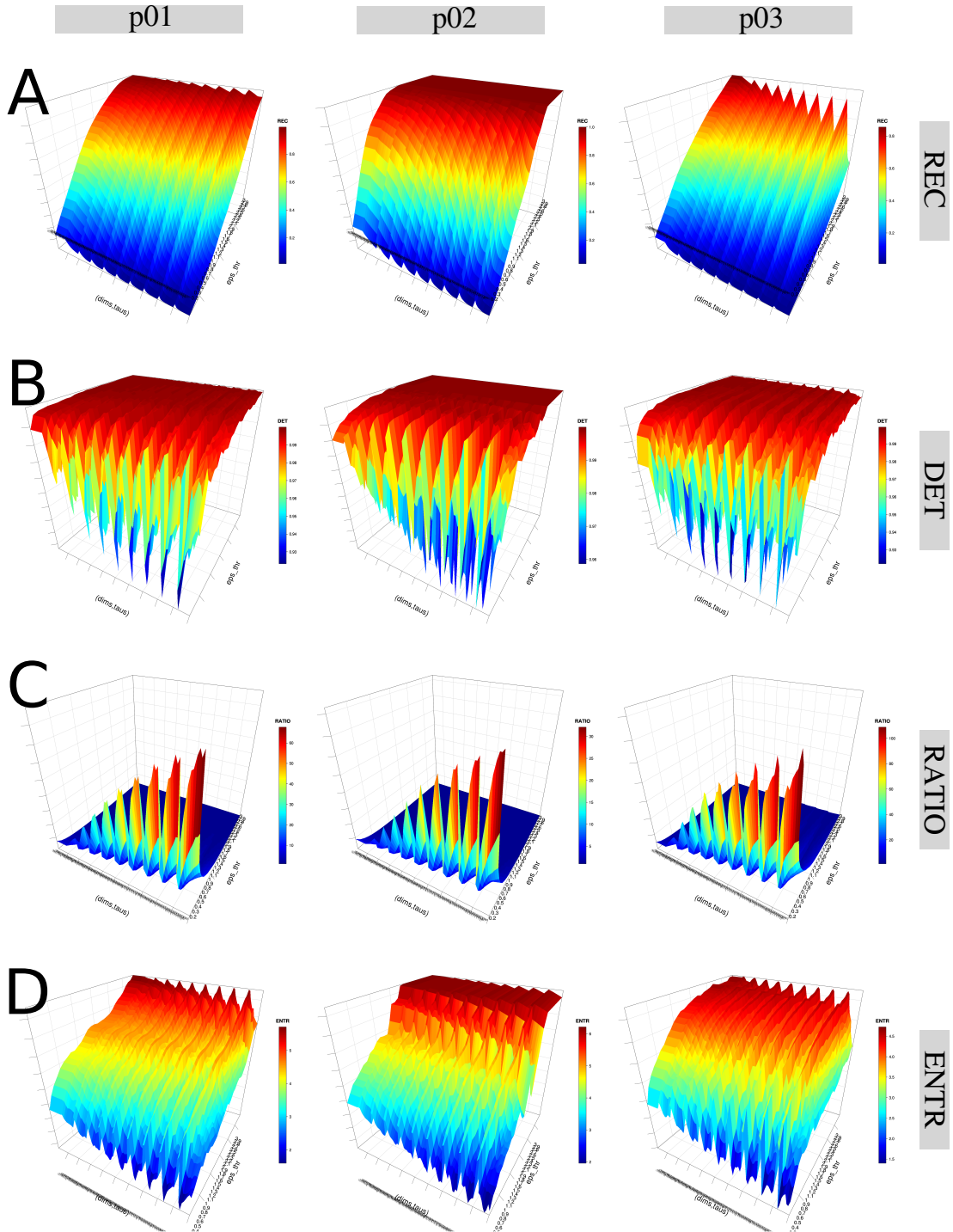


Fig. 6.24 3D surfaces for RQA metrics with three participants. 3D surfaces of RQA metrics ((A) REC, (B) DET, (C) RATIO, and (D) ENTR) for participants *p01*, *p02* and *p03* with increasing embedding parameters and recurrence thresholds. RQA metrics values are for time series of HS01 sensor, HN activity and 500 samples window length. R code to reproduce the figure is available from Xochicale (2018).

